Experimental and Theoretical Study of Low-Cost Hydrothermally Grown Nanowire Silicon Solar Cell

Hung-Hsien Li, Albert S Lin, Yan-Kai Zhong, Sze-Ming Fu, Shih-Yun Lai, Chi-Wei Tseng, Shang-Ru Lin, Wei-Ming Lai, Yu-Chiun Lin, Yu-Ren Li, and Huang-Chung Cheng

Department of Electronic Engineering, National Chiao-Tung University, Hsinchu, Taiwan 30010

***Abstract* — The low cost and high absorbance is the two most important considerations for thin-film silicon photovoltaics. In this work, aluminum doped zinc oxide(AZO) nanowire is grown by low cost hydrothermal method and nano-structured amorphous silicon(α-Si) solar cell is realized on these AZO nanowire substrate. The experimental result shows superior light trapping property compared to conventional planar structure with 18.83% improvement in photocurrent. Simulation result shows the required thickness for full absorption for high aspect ratio AZO nanowire solar cell is ~0.3 m, much thinner than planar type solar cell. The calculation reveals that solar cell absorbance increases with the nanowire length and packing density, indicating material volume is the first order effect for nanowire solar cells. The proposed low-cost AZO nanowire array amorphous silicon solar cell is very promising for future nanostructured silicon photovoltaics.**

***Index Terms* —Nanowire, photovoltaic cells, silicon, light trapping.**

I. Introduction

Light trapping for thin film photovoltaics is very critical for reduced thickness and enhanced absorbance silicon solar cell[1-30]. Nano-structured solar cell is a way to exceed absorption enhancement limit achievable by conventional grating based planar solar cell[15, 31, 32]. This is due to the fact that photons propagate in the direction perpendicular to the film deposition direction so that very thin absorber layer can absorb significant portion of solar photons. Here low cost aluminum doped zinc oxide(AZO) nanowire(NW) solar cell synthesized using hydrothermal method is proposed to realize nanostructured high aspect ratio solar cell. The low temperature hydrothermal process is the key to reduce the cost per watt and the experimental and theoretical result shows significantly improved light trapping property for AZO nanowire solar cell.

II. Simulation of Nano-wire Array Solar Cell

Fig. 1 illustrates the unit cell of aluminum doped zinc oxide(AZO) nanowire array. The light trapping property is enhanced by the periodic arrangement of AZO nanorods, which can actually be regarded as photonic crystal(PC) slab like structure. The high aspect ratio of nanowire provides additional advantage of more material volume where only thin amorphous silicon(α-Si) layer is necessary to fully absorb solar photons. The detailed calculation procedure can be found in literature[27, 33-35].

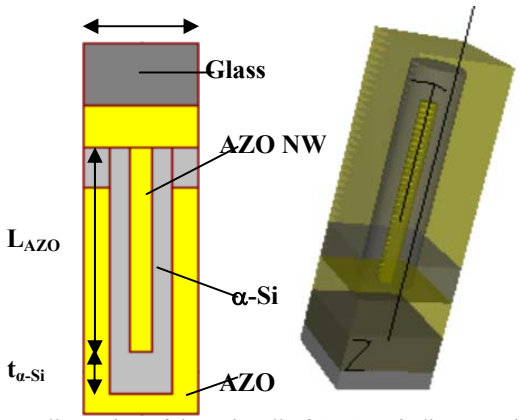

Fig. 1 Illustration of the unit cell of AZO periodic nanowire array.

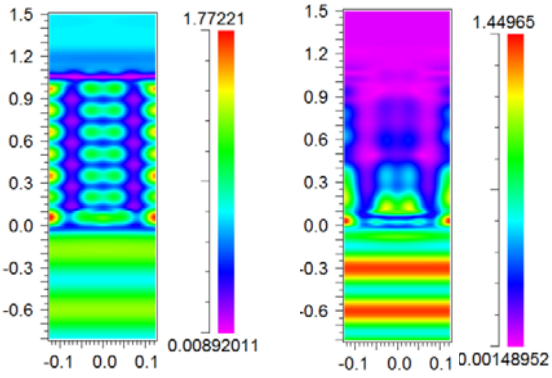

Fig. 2 The field profile cut along nanowire direction for (Left)λ=0.85μm (Right)λ=0.6μm.

The filed profile in Fig. 2 plots the x-component of electric field at harmonic steady state for nanowire solar cell for L_{AZO}=1μm and $t_{α\text{-}Si}$=100nm. In this work, P=0.25μm, and AZO Nanowire diameter is 100nm. At long wavelength, the field penetrates into the entire nanowire structure, forming standing wave pattern. The field intensity at α-Si region is enhanced by periodic nanowire arrangement, leading to quasi-guided mode excitation. Compared to conventional grating based planar structure, high aspect ratio nano-structured solar cell provides better light trapping in the sense that the photons are propagating in the vertical direction and

the active layer thickness can be effectively reduced. For short wavelength, the high absorption coefficient of amorphous silicon results in fast decay of incident field, and the periodic nanowire array acts like anti-reflection coating. The dual roles of nanowire arrays, i.e. light trapping and anti-reflection coating, are more difficult to achieve by grating based geometry.

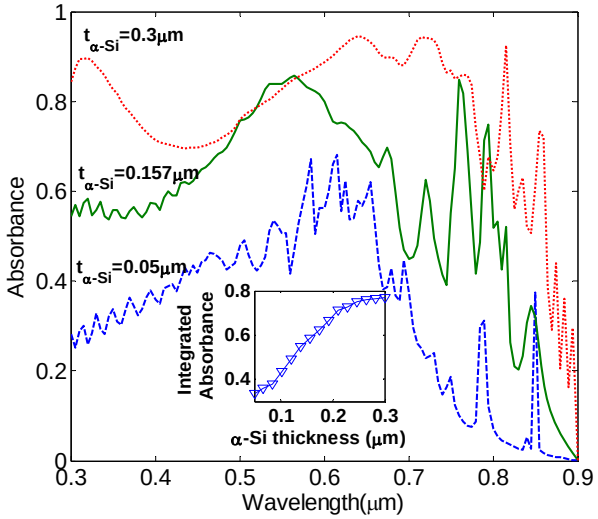

Fig. 3 Spectral response for periodic AZO nanowire solar cell for varying α-Si active layer thickness. L_{AZO}=1 μm.

Fig. 3 shows the spectral response together with the integrated absorbance in the inset calculated by weighting spectral absorbance by AM1.5 solar spectrum. The AZO nanowire length L_{AZO} is 1 μm. The required amorphous silicon thickness is around 0.3μm to achieve full absorption. Note that in the present structure there is no back reflector. The spacing and the width of aluminum stripes at the back side of solar cell is in the order of 50μm so that the light trapping and reflection will not be provided. The experimental J-V is calculated by excluding the area shadowed by aluminum stripes. The superior light trapping property, evident from the thin active layer thickness for saturated absorption, is very promising for future silicon photovoltaics. Using low cost hydrothermal synthesis for AZO nanowire growth further reduces the cost per watt. At long wavelength, the significant quasi-guided mode excitation is identified, which is the result of incident photons coupling into Bloch propagation modes in AZO NW photonic crystal structure.

Fig. 4 shows the spectral response and integrated absorbance for varying AZO nanowire length L_{AZO}. The amorphous silicon layer thickness $t_{\alpha\text{-}Si}$=0.15 μm. The result reveals that with increased L_{AZO}, the efficiency first increases and then saturate. For thicker α-Si thin film thickness, the saturation will be achieved at shorter AZO nanowire length. The result is intuitively correct since with increased NW length, more α-Si material exists. This also indicates the material volume consideration, i.e. more absorbing material for higher absorbance, is the first order effect in nanowire solar cell.

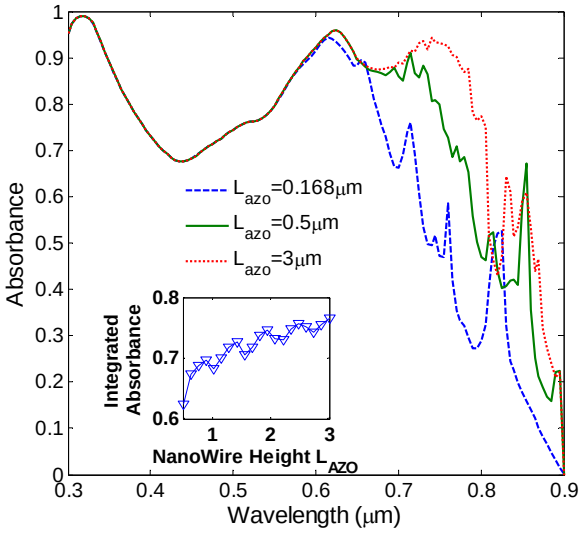

Fig. 4 Spectral response for periodic AZO nanowire solar cell for varying AZO nanowire length L_{AZO}. $t_{\alpha\text{-}Si}$=0.15 μm.

III. Initial Experimental Realization

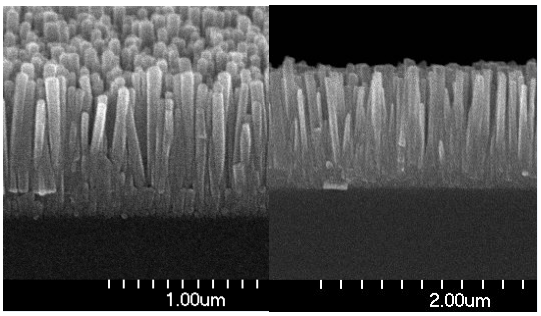

Fig. 5 The SEM micrograph of AZO nanowire array solar cell.

Fig. 5 is the SEM micrograph for AZO nanowire array. Fig. 6 illustrates the fabrication steps. A 200-nm-thick AZO film was deposited on a glass substrate via magnetron sputtering as the seed layer for AZO-nanowire growth. The precursor solution was prepared by mixing 0.025-M zinc nitrate hexahydrate (Zn(NO3)2 · 6H2O) and 0.025-M hexamethylenetetramine in deionized water. Aluminum nitrate nonahydrate (Al(NO3)3 · 9H2O) was then added to the precursor solution to enhance the ZnO-nanowire conductivity. The atomic ratio of Al to (Al+Zn) in the mixing solution was controlled at 3 at%. After the solution was stirred for 15 min, AZO-nanowire growth was carried out at 85◦ C in a quartz beaker placed in a kettle. The growth time

was controlled from 0.5 to 5 h. Finally, the glass substrate was removed from the solution, rinsed with deionized water, and then dried. The AZO wire length was 1–2 μm. After the hydrothermal growth, n-i-p α-Si was sequentially deposited onto the surface of the AZO nanowires using plasma enhanced chemical vapor deposition (PECVD). The PECVD growth conditions were using SiH_4 (10 sccm) source gas at a growth temperature of 350°C, the H_2 dilution ratio $R(H_2/SiH_4)$ = 10, a deposition pressure of 1000 mtorr, a radio frequency of 13.56 MHz, and a plasma power density of 0.08 W/cm2. PH_3 (40 sccm) and B_2H_6/CH_4 (40/40 sccm) were utilized for n-and p-doping. The thicknesses of the p-type and n-type layers were both 30 nm, and the thickness of the intrinsic Si layer varied from 25 to 250nm. A 100-nm-thick AZO layer, which served as a transparent conduction layer, was deposited by sputtering at room temperature. Finally, a 1-μm-thick Al grid, which served as the electrode, was deposited using an electron-gun evaporator. A schematic diagram of the coaxial-structured α-Si *p-i-n* solar cell with AZO nanowires is shown in Fig. 6.

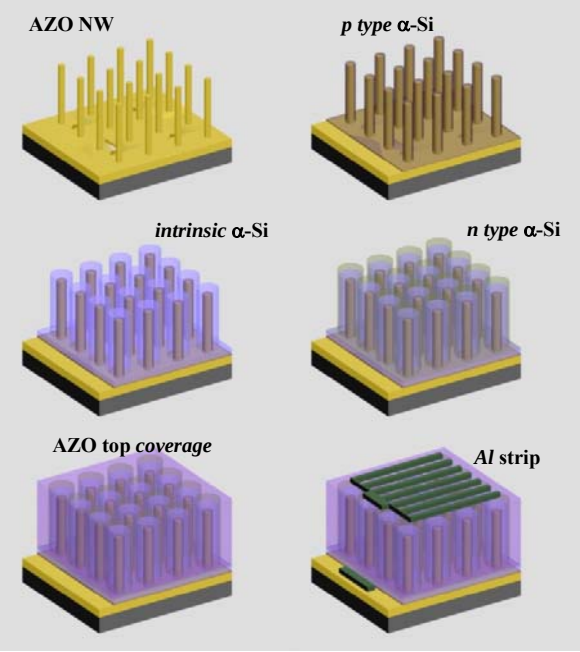

Fig. 6 Illustration of fabrication steps of AZO nanowire solar cell.

Fig. 7 shows the dependence of open circuit votlage, V_{OC}, on nanowire length L_{AZO} for nanowire solar cell. The V_{OC} of planar solar cell is constant around 0.815V. For AZO nanowire solar cell, as L_{AZO} increases, V_{OC} degrades. The degradation of V_{OC} is not very significant and is 3.53%. In practice the length of AZO nanowire is not necessarily to be as long as 2μm to achieve full absorption, provided α-Si thickness can be increased without the drawback of degraded charge collection. The physical reason for degraded V_{OC} is primarily due to the worsened film quality of α-Si desposited on high aspect ration nanowired substrate, which leads to lower mobility and higher defect density. Another reason for lower V_{OC} can be attributed to the fact that carrier transport is also degraded in two dimensional high aspect ratio potential profile of nanowired structure. The current voltage characteristics of AZO nanowire solar cell is shown in Fig. 8. The short circuit current density, J_{SC} increases with the intrinsic layer thickness of *p-i-n* solar cell and has the peak value around 150nm. As the thickness of film is increased beyond 200nm, J_{SC} begins to decrease due to degraded charge collection efficiency. The quality of the amorphous silicon can thus be further improved in order to increase the mobility and to extend the recombination lifetime in intrinsic layer. Once the film quality is improved, the *i*-layer thickness can be increased without sacrificing charge collection and higher photocurrent can be achieved. The improvement of deposited amorphous silicon film quality is currently in progress.

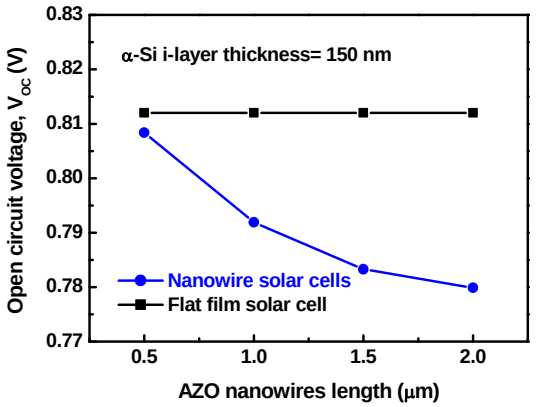

Fig. 7 The dependence of V_{OC} on AZO nanowire length L_{AZO}.

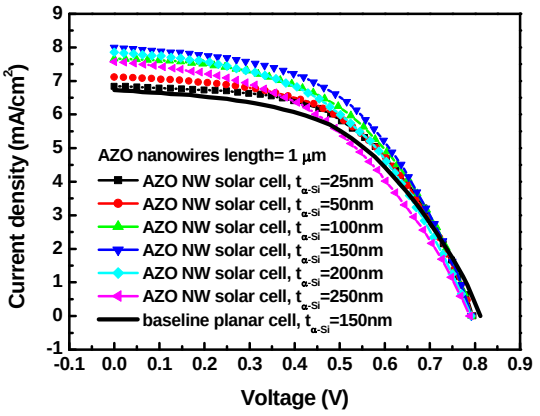

Fig. 8 Current voltage characteristics of AZO nanowire solar cell

VI. Conclusion

The low cost nanowire silicon solar cell is realized using hydrothermally grown AZO nanowires. The result shows the required thickness for amorphous silicon absorber layer is significantly reduced to ~0.3 μm for achieving full absorption, much thinner than conventional planar structure. The calculation reveals that the solar cell absorbance increases with the nanowire length and packing density, indicating the material volume is the first order effect for the photocurrent enhancement of nanowire solar cell. The initial experimental result confirms the superior light trapping by showing 18.83% improvement in J_{SC}. The V_{OC} reduction for high aspect ratio nanowire solar cell is 3.53%. Future effort will be the optimization of silicon film deposition condition to improve the film quality and carrier mobility, which in turn can increase J_{SC} of amorphous silicon solar cell to ideal value.

References

[1] V. Shah, *et al.*, "Thin-film silicon solar cell technology," *Prog. Photovolt. Res. Appl.* , vol. 12, pp. 113–142 2004.

[2] A. Lin, *et al.*, "An optimized surface plasmon photovoltaic structure using energy transfer between discrete nano-particles," *Opt. Express,* vol. 21, pp. A131-A145 2013.

[3] K. Q. Le, *et al.*, "Comparing plasmonic and dielectric gratings for absorption enhancement in thin-film organic solar cells," *Opt. Express,* vol. 20, pp. A39-A50, 2012.

[4] C. Battaglia, *et al.*, "Light Trapping in Solar Cells: Can Periodic Beat Random?," *ACS Nano.,* vol. 6, pp. 2790-2797, 2012.

[5] Z. Yu and S. Fan, "Angular constraint on light-trapping absorption enhancement in solar cells," *Applied Physics Letter,* vol. 98, p. 011106, 2011.

[6] M. Yang, *et al.*, "Incident angle dependence of absorption enhancement in plasmonic solar cells," *Optics Express,* vol. 19, pp. A763-A771, 2011.

[7] P. C. Tseng, *et al.*, "Antireflection and light trapping of subwavelength surface structures formed by colloidal lithography on thin film solar cells," *Prog. Photovolt. Res. Appl.,* vol. 20, pp. 135-142, 2011.

[8] X. Sheng, *et al.*, "Optimization-based design of surface textures for thin-film Si solar cells," *Optics Express,* vol. 19, pp. A841-A850, 2011.

[9] W. E. I. Sha, *et al.*, "Angular response of thin-film organic solar cells with periodic metal back nanostrips," *Opt. Lett.,* vol. 36, pp. 478-480, 2011.

[10] S. Pillai, *et al.*, "The effect of dielectric spacer thickness on surface plasmon enhanced solar cells for front and rear side depositions," *J. Appl. Phys.,* vol. 109, pp. 073105-1-073105-8, 2011.

[11] U. W. Paetzold, *et al.*, "Design of nanostructured plasmonic back contacts for thin-film silicon solar cells," *Opt. Express,* vol. 19, pp. A1219-A1230, 2011.

[12] U. W. Paetzold, *et al.*, "Plasmonic reflection grating back contacts for microcrystalline silicon solar cells," *Appl. Phys. Lett.,* vol. 99, p. 181105, 2011.

[13] A. Naqavi, *et al.*, "Understanding of photocurrent enhancement in real thin film solar cells: towards optimal one-dimensional gratings," *Opt. Express,* vol. 19, p. 140, 2011.

[14] J. N. Munday and H. A. Atwater, "Large Integrated Absorption Enhancement in Plasmonic Solar Cells by Combining Metallic Gratings and Antireflection Coatings," *Nano Lett.,* vol. 11, pp. 2195–2201, 2011.

[15] H.-H. Li, *et al.*, "A Novel Coaxial-Structured Amorphous-Silicon p-i-n Solar Cell With Al-Doped ZnO Nanowires," *Elecron Dev. Lett.,* vol. 32, pp. 928-930, 2011.

[16] N. Lagos, *et al.*, "Theory of plasmonic near-field enhanced absorption in solar cells," *Appl. Phys. Lett.,* vol. 99, p. 063304, 2011.

[17] F.-J. Haug, *et al.*, "Resonances and absorption enhancement in thin film silicon solar cells with periodic interface texture," *J. Appl. Phys.,* vol. 109, p. 084516, 2011.

[18] Y.-J. Chang and Y.-T. Chen, "Broadband omnidirectional antireflection coatings for metal-backed solar cells optimized using simulated annealing algorithm incorporated with solar spectrum," *Opt. Express,* vol. 19, No. S4, pp. A875-A887, 2011.

[19] F. J. Beck, *et al.*, "Light trapping with plasmonic particles: beyond the dipole model," *Opt. Express,* vol. 19, pp. 25230-25241, 2011.

[20] S. Zanotto, *et al.*, "Light trapping regimes in thin-film silicon solar cells with a photonic pattern," *Opt. Express,* vol. 18, pp. 4260-4274, 2010.

[21] Z. Yu, *et al.*, "Fundamental limit of light trapping in grating structures," *Opt. Express,* vol. 18, pp. A366-A380, 2010.

[22] K. Söderström, *et al.*, "Photocurrent increase in n-i-p thin film silicon solar cells by guided mode excitation via grating coupler," *Appl. Phys. Lett.,* vol. 96, p. 213508, 2010.

[23] S. Pillai and M.A.Green, "Plasmonics for photovoltaic applications," *Sol. Energ. Mat. Sol.,* vol. 94, pp. 1481–1486, 2010.

[24] H. Sai, *et al.*, "Light trapping effect of submicron surface textures in crystalline Si Solar Cells," *Prog. Photovolt. Res. Appl.,* vol. 15, pp. 415–423, 2007.

[25] H. Stiebig, *et al.*, "Silicon thin-film solar cells with rectangular-shaped grating couplers," *Prog. Photovolt. Res. Appl.,* vol. 14, pp. 13–24, 2006.

[26] H. Stiebig, *et al.*, "Light trapping in thin-film silicon solar cells by nano-textured interfaces," in *SPIE*, 2006, pp. 619701-1–619701-9.

[27] C. Haase and H. Stiebig, "Optical properties of thin-film silicon solar cells with grating couplers, design and fabrication of submicron grating structures for light trapping in silicon solar cells," *Prog. Photovolt. Res. Appl.* , vol. 14, pp. 629–641, 2006.

[28] N. Senoussaoui, *et al.*, "Thin-film solar cells with periodic grating coupler," *Thin Solid Films* vol. 451–452 pp. 397–401, 2004.

[29] A. Shah, *et al.*, "Photovoltaic technology: the case for thin-film solar cells," *Science,* vol. 285, pp. 692-698, 1999.

[30] M. T. Gale, *et al.*, "Design and fabrication of submicron grating structures for light trapping in silicon solar cells," in *Proceedings of SPIE, Conference on Optical Materials Technology for Energy Efficiency and Solar Energy Conversion IX*, 1990, pp. 60-66.

[31] B. M. Kayes, *et al.*, "Comparison of the device physics principles of planar and radial p-n junction nanorod solar cells," *J. Appl. Phys.,* vol. 97, pp. 114302-1-114302-11, 2005.

[32] L. Tsakalakos, *et al.*, "Silicon nanowire solar cells," *Appl. Phys. Lett.,* vol. 91, pp. 233117-1-233117-3, 2007.

[33] P. Bhattacharya, *Semiconductor optoelectronic devices, 2nd ed.* Upper Saddle River, NJ: Prentice-Hall, 2006.
[34] C. AB, *Comsol multiphysics RF module user guide V 3.3*, 2006.
[35] Synopsys, "Sentaurus device EMW user manual V. X-2005.10," ed, 2005, pp. 78-79.